SCIENCE CHINA Materials ARTICLES

mater.scichina.com link.springer.com

Published online 27 September 2017 | doi: 10.1007/s40843-017-9107-x
Sci China Mater 2017, 60(10): 995–1007

Curcumin-encapsulated polymeric nanoparticles for metastatic osteosarcoma cells treatment

Guanyi Wang[1,2], Wantong Song[2], Na Shen[2], Haiyang Yu[2], Mingxiao Deng[3], Zhaohui Tang[2*], Xueqi Fu[1*] and Xuesi Chen[2]

ABSTRACT **Osteosarcoma is a high-class malignant bone cancer with a less than 20% five-year survival rate due to its early metastasis potential. There is an urgent need to develop a versatile and innoxious drug to treat metastatic osteosarcoma. Curcumin (Cur) has shown its potential for the treatment of many cancers; however, the clinical implication of native curcumin is severely hindered by its intrinsic property. In this study, a mixed system of monomethoxy (polyethylene glycol)-poly(d, l-lactide-co-glycolide)/poly(ε-caprolactone) (mPEG-PLGA/PCL) was used to build a formulation of curcumin-encapsulated nanoparticles (Cur-NPs), which significantly improved the solubility, stability and cellular uptake of curcumin. Moreover, the Cur-NPs were superior to free curcumin in the matter of inhibition on the proliferation, migration and invasion of osteosarcoma 143B cells. It was found that both free curcumin and Cur-NPs could decrease the expressions of c-Myc and MMP7 in the level of mRNA and protein, which explained why free curcumin and Cur-NPs could inhibit the proliferation and invasion of metastatic osteosarcoma 143B cells. The Cur-NPs provided a promising strategy for metastatic osteosarcoma treatment.**

Keywords: curcumin, drug delivery, PLGA, metastatic, osteosarcoma

INTRODUCTION

Osteosarcoma, a malignant bone neoplasm, mainly derives from genetic and epigenetic transformation along with locally aggressive development and early metastatic lesions [1]. Osteosarcoma, which frequently locates and occurs in the regions of distal femur and proximal tibia, brings about a high incidence especially among adolescents. The combination of traditional chemotherapy and surgical intervention is usually used for the treatment of osteosarcoma. However, the application of chemotherapy is often limited due to drug-resistance and severe side effects, which results in disappointing preclinical and clinical outcome [2–4]. Patients bearing osteosarcoma suffer from a very poor cure rate, and the majority eventually die of pulmonary metastases. The five-year survival rate is less than 20% for patients with osteosarcoma [1,5]. Consequently, there is an urgent need to develop a high efficacious and innoxious drug for the treatment of metastatic osteosarcoma.

Curcumin (diferuloylmethane), a polyphenolic chemical constituent isolated from the rhizome of the flora turmeric or *Curcuma longa*, has shown to be able to inhibit the proliferation of a variety of tumor cells in culture and the growth of various human tumors in animal models [6,7]. Several Phase I and Phase II clinical trials using curcumin are undergoing for the treatment of a wide range of tumor types [8,9]. However, native curcumin has low solubility, physicochemical instability, poor bioavailability, rapid metabolism, and poor pharmacokinetics, which can severely hinder the clinical implication of native curcumin [7]. Fortunately, nanocarrier-based delivery systems have shown great potential to overcome these issues [10–12].

Curcumin can inhibit the proliferation of a series of osteosarcoma cells, including MG63 [13–15], U2OS [15–20], MNNG/HOS [21], and KHOS [22], according to literature reports. However, a question remained to answer is whether the curcumin is valid for the treatment of highly metastatic human osteosarcoma. For instance, the 143B is a highly tumorigenic and metastatic human osteosarcoma cell line. Luu *et al.* [23] found that the number of pulmonary metastases was 50-fold higher in 143B injected mice than those injected with MNNG/

[1] Edmond H. Fischer Signal Transduction Laboratory, School of Life Sciences, Jilin University, Changchun 130012, China
[2] Key Laboratory of Polymer Ecomaterials, Changchun Institute of Applied Chemistry, Chinese Academy of Sciences, Changchun 130022, China
[3] College of Chemistry, Northeast Normal University, Changchun 130024, China
[*] Corresponding authors (emails: fxq@jlu.edu.cn (Fu X); ztang@ciac.ac.cn (Tang Z))

HOS. Therefore, it would make sense to investigate the influence of curcumin on 143B cells.

Amplification and overexpression of c-Myc and MMP7 are a common event in various types of cancer cells, including osteosarcoma [24]. The c-Myc protein, a strong proto-oncogene, is helix-loop-helix leucine zipper phosphoprotein that regulates gene transcription in cell proliferation, differentiation and programmed cell death [25,26]. The published articles have reported that the suppression of the c-Myc could induce the cellular senescence [27], and also be associated with the depression of cell proliferation and malignant transformation [28]. MMP7, known as matrilysin, is a member of the matrix metalloproteinase (MMP) family [29]. In human cancer cells, MMP7 seems to be unique among MMPs because it is mainly produced by the cancer cells themselves and not solely by stromal cells as other MMPs. Increased level of MMP7 was correlated with the presence of metastasis and poor patients' survival in colorectal, bladder and renal cell cancer [30]. This kind of matrix-degrading enzyme, MMP7, contributes to the invasion of many types of malignant cancer cells [31–33]. Down regulation of c-Myc and MMP7 is thought to be an effective method to inhibit the proliferation and prevent the invasion of cancer cells [30,32,34]. It will be interesting to investigate the expression of c-Myc and MMP7 proteins in highly invasive 143B cells with the treatment of curcumin.

In this study, we utilized a mixed system of monomethoxy (polyethylene glycol)-poly(d, l-lactide-co-glycolide)/poly(ε-caprolactone) (mPEG-PLGA/PCL) with low critical aggregation concentration (CAC) for the encapsulation of curcumin. The formed curcumin-loaded nanoparticles (Cur-NPs) were characterized in detail. The ability of the Cur-NPs to inhibit the proliferation and prevent the invasion 143B cells were investigated and compared with free curcumin. The influence of the treatment of free curcumin and Cur-NPs on the expression of c-Myc and MMP7 proteins in 143B cells was also studied.

EXPERIMENTAL SECTION

Materials

mPEG-PLGA (molecular weight (M_w): mPEG 5000 Da, PLGA 2000 Da, d,l-LA/GA 75/25) and PCL (M_w: 3400 Da) were given by Changchun Sinobiomaterials Co., Ltd., China as a gift. Curcumin was purchased from Sigma-Aldrich. Other reagents and solvents were purchased from Sinopharm Chemical Reagent Co. Ltd. and used as received.

Preparation of the nanoformulation and characterization

The mPEG-PLGA (30 mg), PCL (60 mg) and curcumin (10 mg, purity>98%) were dissolved in 2.0 mL of *N*,*N*'-dimethylformamide/acetonitrile (DMF/CH_3CN, 1/1, *v*/*v*). The above solution was added dropwise to 2.0 mL MilliQ water under mild stirring. After agitation for 1 h, the mixture was transferred into a dialysis bag (MWCO 3500Da) and dialyzed for 36 h to remove organic solvent and free curcumin. The mixture in the dialysis bag was centrifuged at 8000 rpm for 5 min and then filtered through a syringe filter (membrane filter 0.45 μm). The filtered solution was the expectant Cur-NPs which was kept at 4°C before use or lyophilized with 4% injection-grade trehalose.

The particle size distribution of the obtained Cur-NPs was investigated by dynamic light scattering (DLS) using a Wyatt-QELS instrument with a vertically polarized He-Ne laser (DAWN EOS, Wyatt Technology) at 90° collecting optics. Transmission electron microscopy (TEM) measurement was performed on a JEOL JEM-1011 transmission electron microscope with an accelerating voltage of 100 kV. The measurement of CAC of the Cur-NPs was carried out on a fluorescence spectroscopy using pyrene as a probe on a fluorescent detector (PTI, Photon Technology International, Inc.), following our previously published method [35,36].

The content of curcumin entrapped in Cur-NPs was determined using a high-performance liquid chromatography (HPLC), consisting of a reverse-phase C-18 column (symmetry), with a mobile phase of acetonitrile/5% acetic acid (55/45, *v*/*v*) pumped at a flow rate of 1.0 mL min^{-1}. Detection was taken on a Waters 2475 multi λ detector and the detection wave-length for curcumin was set at 425 nm. The drug loading content (DLC %) and drug loading efficiency (DLE%) were calculated by the following:

$$\mathrm{DLC\%} = \frac{\text{Cur amount}}{\text{total NPs amount}} \times 100\%, \quad (1)$$

$$\mathrm{DLE\%} = \frac{\text{Cur content in NPs}}{\text{theoretial Cur content in NPs}} \times 100\%. \quad (2)$$

In vitro drug release study

A modified dialysis method was used to study the *in vitro* release behavior of curcumin from the Cur-NPs. In brief, 3.0 mL Cur-NPs solution (containing 0.324 mg curcumin) was placed in a dialysis bag (MWCO 3500 Da), which was then incubated in 50 mL of phosphate buffered saline (PBS, pH 7.4 or pH 5.5) containing Tween80 (0.05 wt.%) with gentle shaking (100 rpm) at 37°C. At each specific time (2, 4, 6, 8, 10, 12, 24, 36, 48, 72 h), every

3 mL release media were collected and replaced by fresh media. The collected release media was filtered through a 0.22 μm syringe filter membrane, and the amount of curcumin in the filtrate was determined by HPLC.

Stability test of the Cur-NPs and free curcumin

The Cur-NPs or free curcumin (dissolved in dimethyl sulphoxide (DMSO) and diluted by using water or PBS) were placed in a 37°C horizontal vibrator at a shaking rate of 100 rpm. The original concentration is 0.01 mg mL^{-1} equivalent curcumin in water or PBS (37°C, pH 7.4) containing 10% fetal bovine serum (FBS). At particular time point (0, 6, 12, 24, 48, 72, 96 h), a 0.5 mL aliquot of the solution was withdrawn, freeze-dried, and the curcumin content was measured by HPLC. Residual Cur (%) was calculated by comparing with the initial curcumin concentration.

The nanoparticle sizes and intensities of Cur-NPs in water or PBS with 10% FBS at particular time point (0, 6, 12, 24, 48, 72, 96 h) were tested by DLS according to the above method. The original concentration is 0.5 mg mL^{-1} equivalent curcumin.

Cell culture

The human osteosarcoma cell line 143B, purchased from North Carolina Chuang Lian Biotechnology Research Institute (Beijing, China), was cultured in RPMI 1640 medium supplemented with 10% FBS, 100 U mL^{-1} penicillin and 100 U mL^{-1} streptomycin at 37°C in a humid incubator with 5% carbon dioxide.

Cytotoxicity assay

The cytotoxicity of free curcumin and Cur-NPs towards 143B cells was determined by MTT (3-[4,5-dimethylthiazol-2-yl]-2,5 diphenyl tetrazolium bromide) assay. Cells were seeded in 96-well plates at a density of 6000 cells per well. After 24 h incubation, free curcumin or Cur-NPs were added into the culture medium at predefined concentrations. The 143B cells were incubated for another 24 or 48 h. The MTT solution (20 μL, 5.0 mg mL^{-1}) was added into each well. The plates were incubated for 4 h at 37°C. After the medium was gently removed by pipette, 150 μL of DMSO was added, and the plates were agitated for 5 min to dissolve the formazan dye. The optical density (OD) of each well at 490 nm was measured on a Bio-Rad 680 microplate reader. Data are presented as means ±standard deviation (n=4). The relative cell viability was determined by comparing the OD at 490 nm with control wells containing only cell culture medium. Cell viability (%) was determined according to the following equation:

$$\text{Cell viablity (\%)} = \frac{\text{OD}_{\text{sample}}}{\text{OD}_{\text{control}}} \times 100\%, \quad (3)$$

where, the OD_{sample} and $OD_{control}$ represent for the absorbance of the sample wells and control wells, respectively.

Cellular uptake assay

The 143B cells were seeded into 6 well plates at a density of 1×10^5 cells per well. After 24 h, the medium was replaced with fresh medium containing 20 μmol L^{-1} curcumin or Cur-NPs. The cells were incubated for another 1 or 3 h at 37°C. After the media were removed, the cells were washed three times with cold PBS and fixed with fresh 4% paraformaldehyde for 30 min at room temperature. The coverslips were placed onto the glass microscope slides, and observed on a confocal laser scanning microscope (CLSM, Carl Zeiss LSM 780).

For flow cytometry (FCM) measurement, the 143B cells were seeded onto 6 well plates at a density of 3×10^5 cells per well. The medium was replaced with fresh medium containing 20 μmol L^{-1} curcumin or Cur-NPs after 24 h incubation at 37°C. The 143B cells were incubated for another 1 or 3 h. The culture media were removed. The remained cells were washed three times with cold PBS and collected for FCM measurement.

Colony formation assay

Colony formation assay was used to evaluate the ability of a single cell colony forming one colony [37]. The 143B cells, treated with free curcumin or Cur-NPs (10 or 20 μmol L^{-1}) for 24 h, were seeded into 12-well plates at a density of 3000 cells per well at 37°C in a 5% CO_2 humidified environment. Five days later, the colonies were fixed with 4% paraformaldehyde and stained with 0.5% crystal violet. More than 50 cells were regarded as one colony. The numbers of colonies in each well were counted under an inverted microscope. The cloning efficiency was defined as the ratio of the number of colonies formed to the number of cells seeded ×100%.

Wound-scratch assay

The 143B cells were seeded in a 6-well plate at a density of 1×10^6 cells per well and incubated for 24 h. A pipette tip was used to scratch three perpendicular wounds into a cross shape, and the wells were washed twice with PBS to remove the detached cells and avoid interference. The 143B cells were covered by 10 μmol L^{-1} curcumin or Cur-NPs solution for a corresponding point time. Curcumin or Cur-NPs solution were diluted with medium only containing 1% FBS to eliminate the influence of cell

proliferation. The wounds were photographed using an inverted microscope. The wound closure rate was the percentage of wound closure which is calculated as (original gap distance-gap distance at 12 or 24 h)/original gap distance ×100%.

Transwell invasion assay

Adhesive 143B cells were starved in serum-free medium for 12 h and then re-suspended in serum-free medium with 10 μmol L^{-1} curcumin or Cur-NPs for another 12 h. Then, 5×10^4 cells per well were added to the upper chamber of transwells (6.5 mm diameter inserts, 8.0 μm pore size, polycarbonate membrane, from Costar) precoated with matrigel (eight times dilution by DMEM medium), while the lower chamber was filled with 500 μL of complete culture medium containing 20% FBS as an attractant source. After 12 h of incubation at 37°C, the cells that had invaded towards the lower surface of the membrane were fixed with 4% paraformaldehyde and stained with 0.5% crystal violet. Using light microscopy, five random fields were selected, and the cells in each field were counted under 100× magnification.

Apoptosis analysis

The 143B cells were seeded into 6-well plates and allowed to adhere overnight. When a confluence of 70%–80% was reached, the 143B cells were exposed to 20 μmol L^{-1} curcumin or Cur-NPs for 48 h. Subsequently, the cells were collected and re-suspended in PBS. Annexin V-PE and 7-AAD were added to all of the samples, which were then incubated at room temperature for 5–15 min in the dark according to the manufacturer's protocol from the Annexin V-PE/7-AAD apoptosis detection kit. The fluorescence intensity of every sample was immediately analyzed by flow cytometry.

Real-time quantitative polymerase chain reaction (RT-PCR)

For RT-PCR analysis to quantify gene expression, the method of detection was SYBR Green l. Firstly, 143B cells were treated with 10 and 20 μmol L^{-1} curcumin or Cur-NPs for 48 h. Total RNA of each sample was extracted using RNAprep Pure Cell Kit, then quantified to the same standard and reversely transcribed into cDNA. Finally, the cDNA was added to a 20 μL real-time PCR reaction system on the PCR instrument (Stratagene Mx 3005P, USA) according to the manufacturer's protocol. The detailed information of every primer pair were used in this system for the following genes: C-MYC (F-5′-GTAGTGGAAAACCAGCAGCG-3′, R-5′-AGAAATACGGCTGCACCGAG-3′), MMP7 (F-5′-CTCTCTGGACGGCAGCTATG-3′, R-5′-TAGTCCTGAGCCTGTTCCCA-3′), GAPDH (F-5′-CAATGACCCCTTCATTGACCTC-3',R-5′-AGCATCGCCCCACTTGATT-3′). The PCR amplification was performed under the condition of 1 cycle (95°C for 15 min) and 40 cycles (95°C for 10 s, 60°C for 20 s and 72°C for 32 s). GAPDH was used as an internal reference to verify equal concentration of cDNA in each sample. The whole experimental kits were purchased from Tiangen Biotech Co., LTD, Beijing, China. We applied 2-ΔΔCT method to analyze the outcomes.

Western blot analysis

For protein expression analysis, 143B cells were seeded in 100-mm dishes and treated with curcumin or Cur-NPs (20 μmol L^{-1}) for 48 h, respectively. Total proteins were extracted by Kit according to the manufacturer's protocol. The protein concentration was detected based on the bicinchoninic acid (BCA) method.

All the samples were mixed with 5× sodium dodecyl sulfate (SDS) loaded buffer, boiled for 5 min and stored at −20°C for later use. The samples with same amount protein were separated on a SDS-PAGE gel (10% separation gel) and transferred to a nitrocellulose membrane after electrophoresis. The membranes were blocked with 5% BSA in TBS containing 0.1% Tween20 for 1 h and were incubated waveringly with corresponding rabbit primary antibodies overnight at 4°C. The antibodies included c-Myc, MMP7 (1:500, Abcam), and GAPDH (1:2000, Abclone). Among them, GAPDH were used as an internal control for the total protein. The secondary antibody was a conjugated goat (polyclonal) anti-rabbit IgG antibody (1:10000). Subsequently, the bands were incubated by the secondary antibody for one hour and washed off remnant uncombined antibodies. The reactive bands were covered by electrogenerated chemiluminescence (ECL) developing-coloring solution and visualized with a bio-rad ChemiDoc MP chemiluminescence imaging system.

Statistical analysis

All mean values ± SD reported in results section were compared by student's t test. P values of <0.05 were considered significant, P values of <0.01 considered extremely significant.

RESULTS AND DISCUSSION

Preparation and characterization of the nanoformulations

The Cur-NPs were prepared by the method of nanopre-

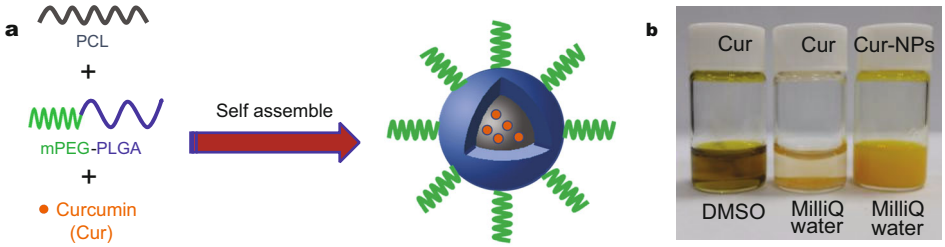

Figure 1 Preparation of Cur-encapsulated mPEG-PLGA/PCL nanoparticles. (a) Schematic diagram of the prepared Cur-NPs; (b) appearance of free Cur in DMSO, free Cur in water, Cur-NPs in water, 2 mg mL^{-1} pure Cur equivalent.

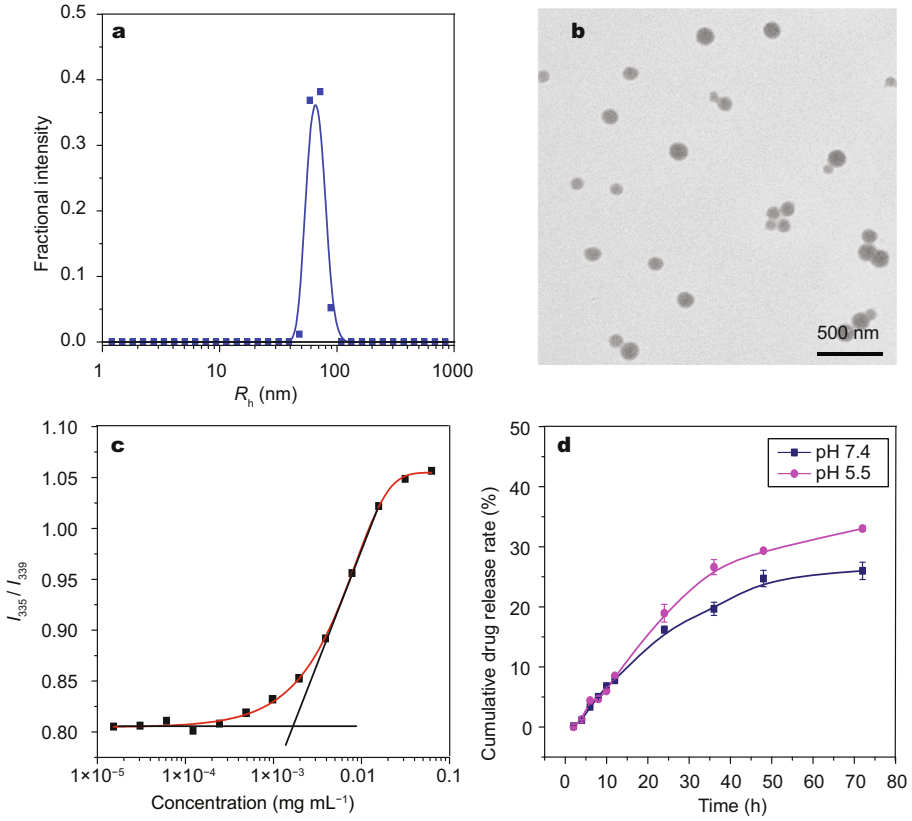

Figure 2 Properties of Cur-NPs. (a) Particle size of Cur-NPs measured by DLS; (b) TEM image of Cur-NPs; (c) CAC; (d) *in vitro* drug release of Cur-NPs.

cipitation. Many literatures have reported that PCL or PLGA could be served as compatible biomaterials to build nanocarrier-based delivery systems [38–40]. Herein, PCL was utilized to stabilize hydrophobic core, while mPEG-PLGA was used to improve the solubility of nanoparticles owing to pegylation [41–45] (Fig. 1a). The mPEG-PLGA/PCL delivery system could solve the hydrophobic problem of curcumin. As shown in Fig. 1b, free curcumin was readily dissolved in DMSO, while most of curcumin was precipitated in water, because free curcumin has low solubility in aqueous solution (approximately 20 μg mL^{-1}) [46]. In contrast, the curcumin-loaded mPEG-PLGA/PCL mixed nanoparticles Cur-NPs could be dissolved in water and form uniform solution, which should be attributed to the pegylation of the nanoparticles improving the water-solubility. The hydrodynamic radius of the Cur-NPs in water determined by DLS is ~66.8 nm (Fig. 2a), which is close to the TEM image results (Fig. 2b). It is well known that nanoparticles with radius less than 100 nm could target passively to solid tumor by the enhanced permeability and retention (EPR) effect [47–49]. The Cur-NPs satisfy the above conditions, and therefore have the po-

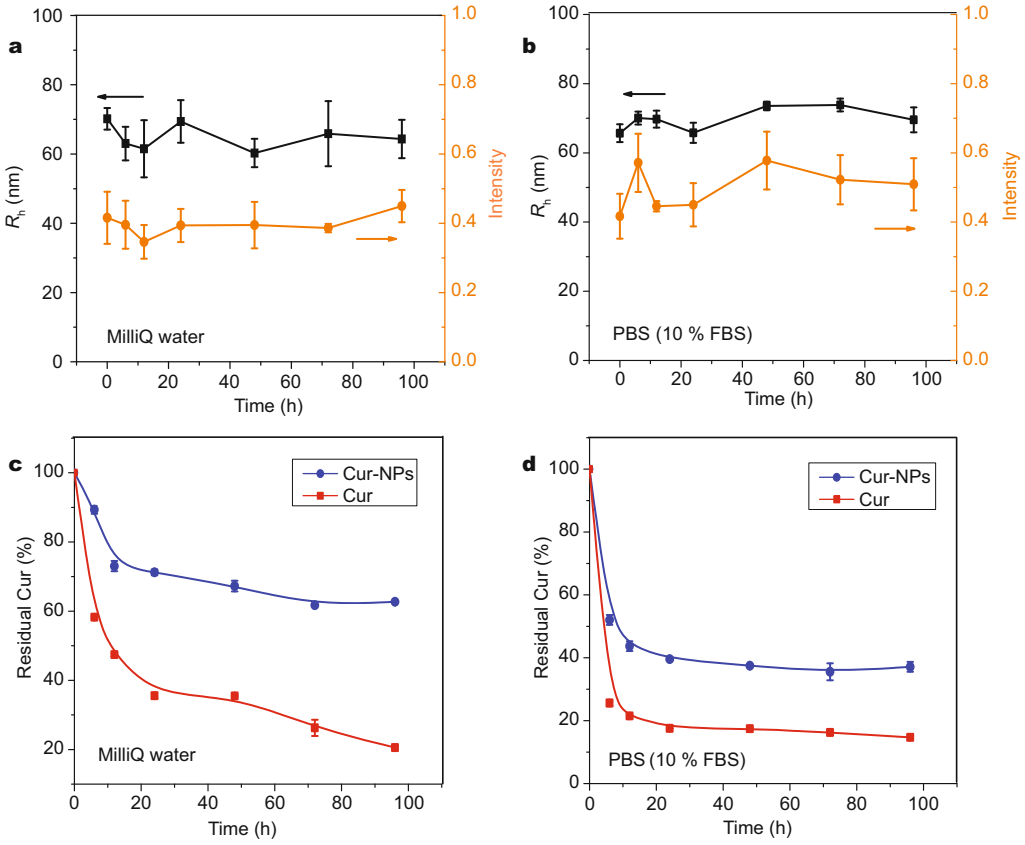

Figure 3 The stability of Cur-NPs and Cur in water and PBS with 10% FBS. (a, b) Particle sizes and intensities of Cur-NPs determined by DLS (n=3); (c, d) residual curcumin of free curcumin (Cur) and Cur-NPs (n=3).

tential for the application in cancer therapy.

The DLC and DLE of the Cur-NPs were 7.3 wt.% and 72.8%, respectively. The curcumin content in the lyophilized Cur-NPs with protectants was 18.8 μg mg^{-1}. The CAC of the Cur-NPs was 1.686×10^{-3} mg mL^{-1} (Fig. 2c). The low value of CAC reflects the high thermodynamic stability, which suggests that the designed drug carrier with lower CAC could accurately deliver to preset location without disintegration in advance.

Curcumin release from Cur-NPs

A burst release behavior of cargo was often observed in the delivery systems of curcumin, which greatly impaired the utilization of curcumin [10,50]. As shown in Fig. 2d, the Cur-NPs show a sustained release without burst release in PBS, pH 7.4. Only 25% curcumin were released from Cur-NPs in 72 h. The slow release *in vitro* could be explained by the high hydrophobicity of PCL stabilizing the core of the Cur-NPs. Because of the slow drug release, the Cur-NPs could have a high chance to accumulate at tumor site by EPR effect. The unreleased curcumin in the Cur-NPs in blood circulation could be taken up by cancer cells through the endocytosis process.

And Cur-NPs had a little higher cumulative curcumin release at pH 5.5 than at pH 7.4, which may be related to a faster degradation of free curcumin at pH 7.4 [51,52]. The enhanced release behavior at a lower pH would highlight its advantages for anti-tumor effects since tumor tissue is inclined to an acidic microenvironment.

Stability of Cur-NPs in aqueous solution

Free curcumin in water would readily be decomposed at physiological pH [51], which is an important reason of the rapid metabolism and poor pharmacokinetics of curcumin. To evaluate the stability of Cur-NPs in aqueous solution, we measured the particle sizes and intensities of the Cur-NPs at different time intervals in water and PBS with 10% FBS by DLS. As shown in Fig. 3a, b, the particle sizes and intensities of the Cur-NPs in water or in PBS with 10% FBS did not change much in 96 h, confirming the stability of Cur-NPs in water and in PBS with 10% FBS without significant dissociation.

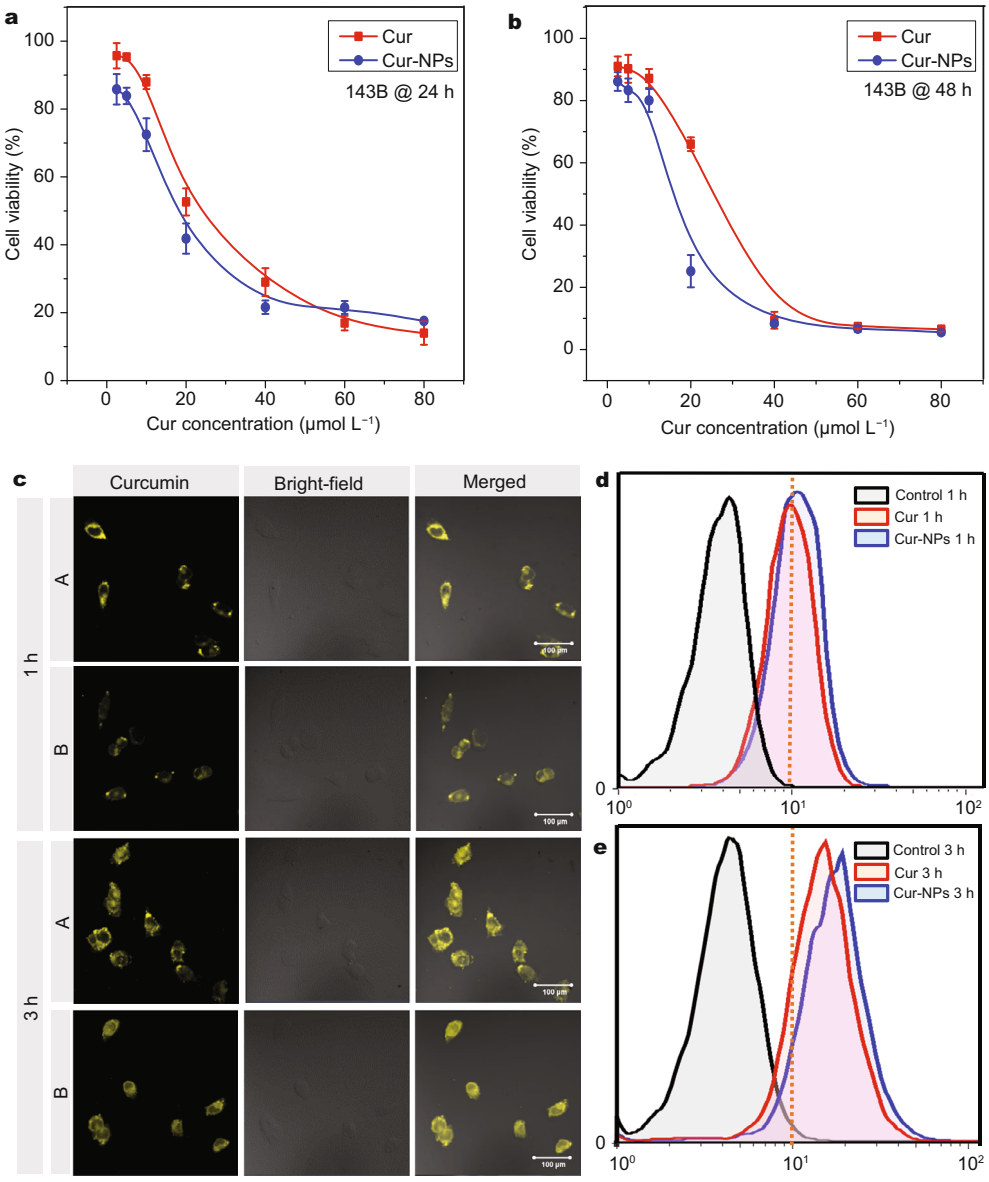

Figure 4 *In vitro* cytotoxicity and cellular uptakes of Cur and Cur-NPs. (a, b) Cytotoxicity of free Cur and Cur-NPs after 24 or 48 h treatment (n=4); (c) CLSM observations (A: Cur, B: Cur-NPs, Scale bars, 100 μm) and (d, e) FCM analysis for cellular uptakes of Cur and Cur-NPs by 143B cells after treatment with free Cur or Cur-NPs for 1 or 3 h.

To further investigate the stability of free curcumin and Cur-NPs, the residual curcumin of free curcumin and Cur-NPs in water or PBS with 10% FBS was measured at different time intervals. As shown in Fig. 3c, d, 80% of free curcumin decomposed in water at 96 h, while in contrast, less than 40% of curcumin in the Cur-NPs decomposed under the identical condition. Similarly, the residual curcumin in the Cur-NPs was about twice as much as the free curcumin in PBS with 10% FBS at 96 h, despite of complicated components in FBS (like some enzymes and surfactants), which could accelerate the degradation and further decrease the stability of the Cur-NPs. These indicate that the Cur-NPs are superior to free curcumin, protecting curcumin from decomposition in physiological environment.

In vitro cytotoxicity of Cur-NPs towards 143B cells

The MTT assay was used to evaluate the cytotoxic effect of free curcumin and Cur-NPs towards 143B cells. Fig. 4a, b show dose- and time- dependent cytotoxicity of free

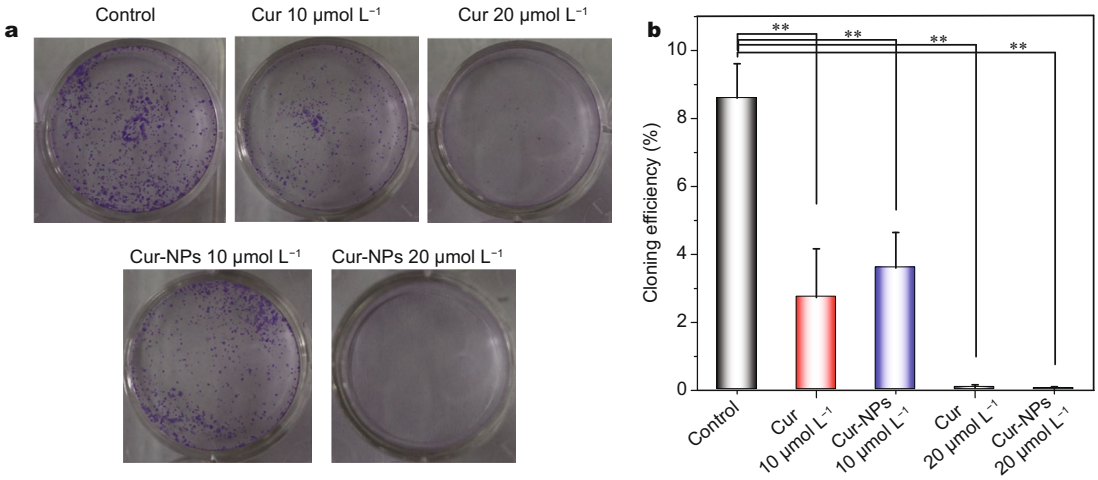

Figure 5 Suppression of colony formation of 143B cells by free Cur and Cur-NPs (n=5). (a) Observations under an inverted microscope; (b) the counted cloning efficiencies (∗ p<0.05, ∗∗ p<0.01).

curcumin or Cur-NPs towards 143B cells at 24 and 48 h. The half inhibition concentration (IC_{50}) of free curcumin or Cur-NPs at 24 h is 21.3 or 16.8 μmol L^{-1}, respectively. The IC_{50} of free curcumin or Cur-NPs at 48 h is 17.9 or 13.1 μmol L^{-1}, respectively. In Fig. 4b, the fitted curves show larger difference between the Cur group and Cur-NPs group at 48 h than at 24 h, which may be attributed to the sustained release and slower degradation of Cur-NPs. The free small molecule curcumin is transported into cells *via* a passive diffusion, while Cur-NPs enter cells mainly by endocytosis [53], indicating that the Cur-NPs possess a higher inhibition for proliferation of 143B cells as compared with free curcumin.

Cellular uptake of Cur-NPs

Since curcumin could emit fluorescence [54], the uptake of curcumin can be visualized by CLSM and FCM. As shown in Fig. 4c, for both free curcumin and Cur-NPs after 1 h incubation, curcumin fluorescence is observed in the 143B cells and most of curcumin is distributed in cytoplasm. For both free curcumin and Cur-NPs after 3 h incubation, the intracellular curcumin fluorescence is stronger than that of 1 h incubation time. Moreover, the curcumin fluorescence is distributed both in cytoplasm and nucleus, demonstrating that curcumin could rapidly act on 143B cell nuclei through nuclear pore. FCM analysis (Fig. 4d, e) shows that the curcumin fluorescence intensity of 143B cells treated with Cur-NPs is stronger than that with free curcumin at both 1 and 3 h, indicating that the uptake of Cur-NPs by 143B cells is more efficient than that of free curcumin.

Suppression of colony formation by Cur-NPs

Colony formation assay is a powerful tool to determine the effectiveness of cytotoxic agents [52]. As shown in Fig. 5a, the curcumin groups, no matter whether free curcumin or Cur-NPs, considerably show less colony formation as compared with the control group. The cloning efficiency of 143B cells is dose-dependent. At 10 μmol L^{-1}, the cloning efficiencies are 2.7% (free curcumin) and 3.6% (Cur-NPs), respectively. At 20 μmol L^{-1}, the cloning efficiencies reduce to 0.07% (free curcumin) and 0.03% (Cur-NPs), respectively (Fig. 5b). For the 143B cells treated by 20 μmol L^{-1} free curcumin or Cur-NPs (equivalent based on curcumin), there are few formed colonies in the plates, indicating that 20 μmol L^{-1} curcumin is enough to prevent the "unlimited" division of 143B cells. It could be conjectured that the 143B cells treated by 20 μmol L^{-1} curcumin might be impaired in respect of forming single colony.

Cur-NPs inhibiting the migration and invasion of 143B cells

Wound-scratch assay was used for the analysis of 143B cell migration *in vitro*. In order not to influence cell survival and inhibit cell proliferation, only 1% FBS was added in the culture medium. After 24 h migration, the scratch wound was closed approximately 70% in the control group, whereas the 143B cells treated with free curcumin and Cur-NPs only narrowed the scratch by 37% and 29%, respectively (Fig. 6a, b). It is worth noting that the wound closure rate of Cur-NPs group is lower than that of free curcumin after 12 or 24 h migration,

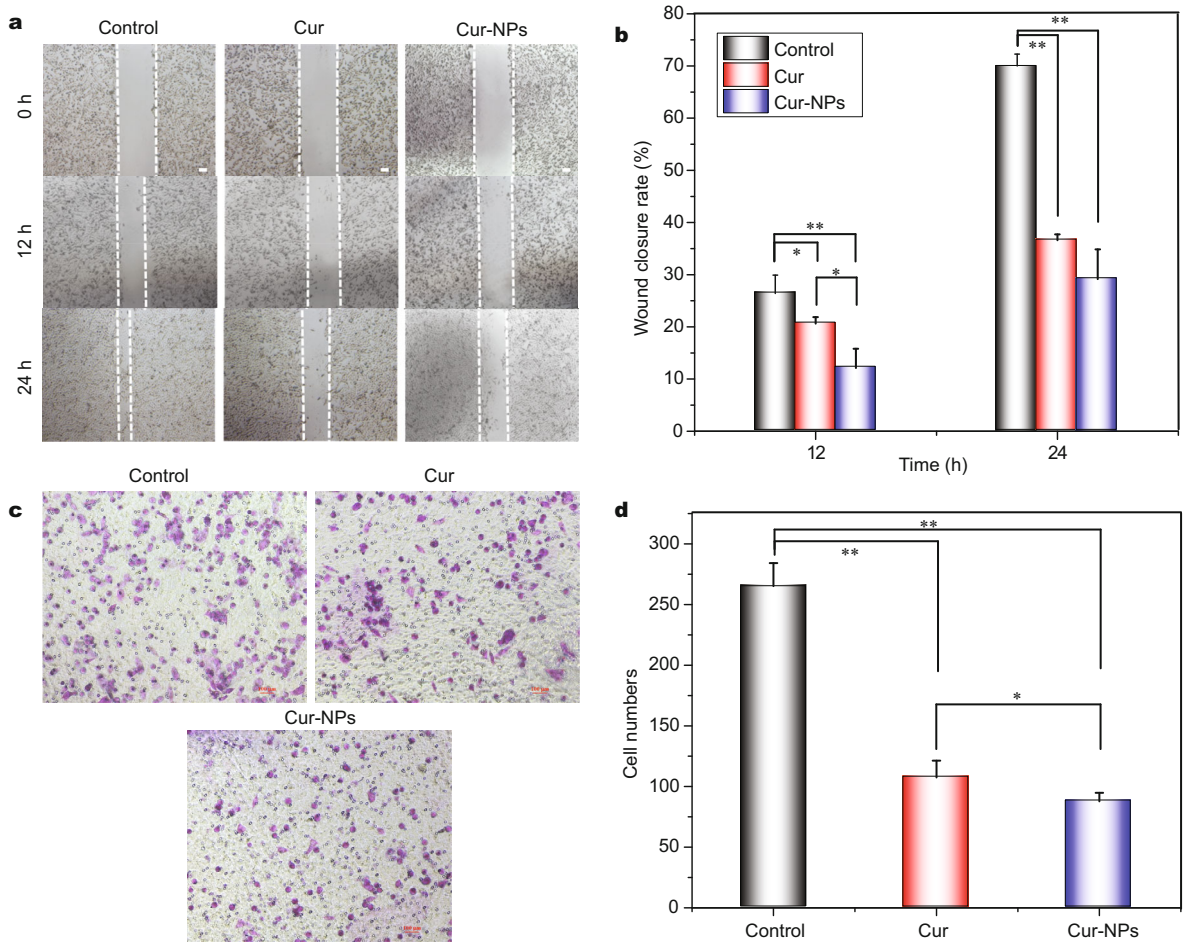

Figure 6 The inhibition effect of Cur and Cur-NPs on cell migration and invasion. (a, b) Inhibitory effect on 143B cells migration by free Cur or Cur-NPs (scale bars, 200 μm; n=3, Mean±SD, ∗ p<0.05, ∗∗ p<0.01); (c, d) changes of 143B cells invasion after treatment with free Cur and Cur-NPs (Scale bars, 100 μm; n=5, mean±SD, ∗ p<0.05, ∗∗ p<0.01).

indicating that the Cur-NPs are more efficient than free curcumin in inhibiting the migration of 143B cells.

The invasion of 143B cells was assessed by Matrigel-based Transwell assay (Fig. 6c, d). Consistent with the wound-scratch assay, in the 12 h transwell assay, the number of invaded 143B cells was extremely significantly reduced in the groups treated with free curcumin or Cur-NPs than that of control group. Likewise, the Cur-NPs showed significantly higher ability to inhibit the invasion of 143B cells than that of free curcumin.

Cell apoptosis triggered by Cur-NPs

The apoptosis of 143B cells was analyzed by FCM. As shown in Fig. 7, Annexin V-PE and 7-AAD were used to differentiate the cells, including early apoptotic cells (bottom right corner), late apoptotic cells (top right corner). Both free curcumin and Cur-NPs' treatment could increase the proportion of apoptotic cells as compared with the control group. The Cur-NPs' treatment induced slightly more late apoptotic cells than the free curcumin (23.7% *vs.* 20.7%), while the proportions of early apoptotic cells were 25.4% (free curcumin) and 21.0% (Cur-NPs), respectively. These results demonstrate that the Cur-NPs could trigger the strong apoptosis of the 143B cells.

Decreased expressions of c-Myc and MMP7 by Cur-NPs

As shown in Fig. 8a, b (RT-PCR analysis) and Fig. 8c (western blotting assay), both free curcumin and Cur-NPs could significantly decrease the expressions of c-Myc and MMP7 in the level of mRNA and protein. The 20 μmol L^{-1} free curcumin displayed a higher inhibition on expressions of c-Myc and MMP7 than 10 μmol L^{-1} in Fig. 8a, b. The Cur-NPs showed a similar inhibitory effect

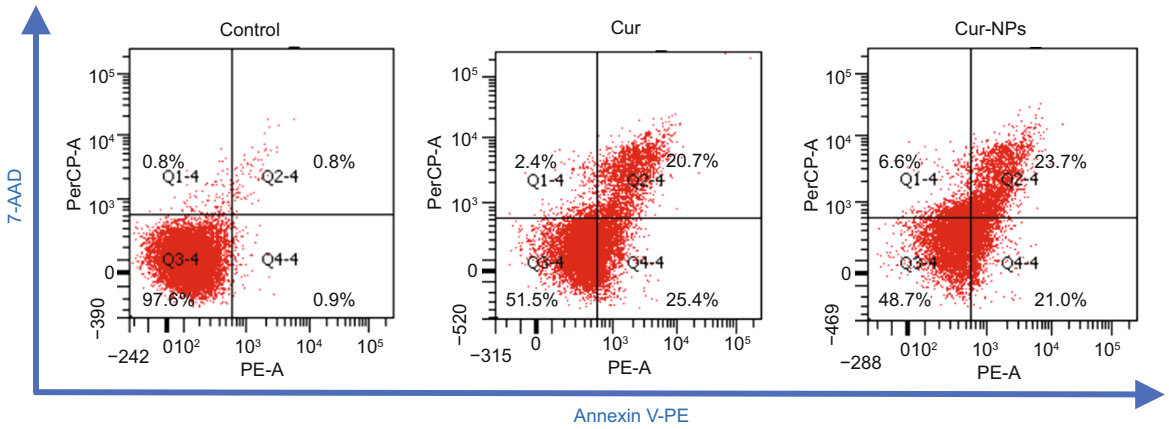

Figure 7 Cell apoptosis analysis of 143B cells by FCM.

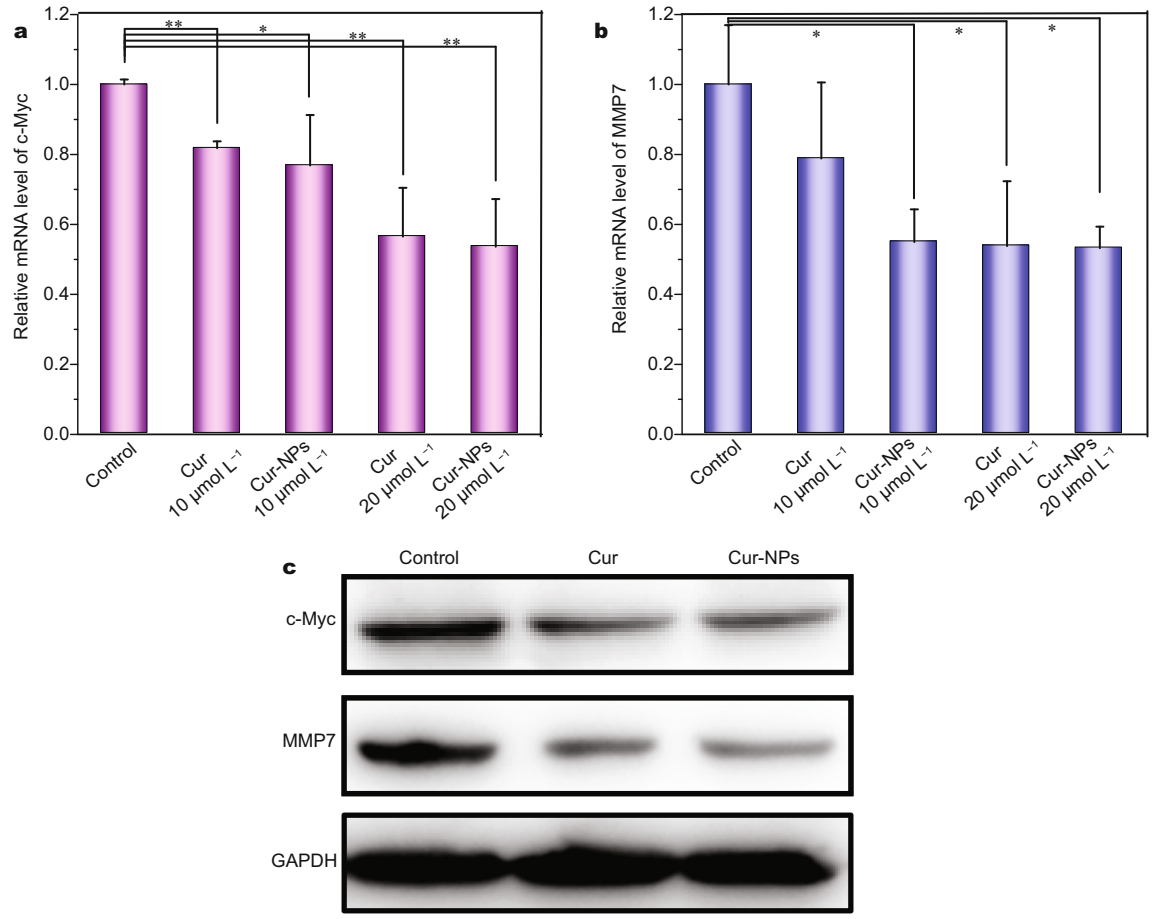

Figure 8 The c-Myc and MMP7 expressions. (a, b) Relative mRNA level of c-Myc and MMP7; (c) western blotting of c-Myc protein and MMP7 protein (∗ $p<0.05$, ∗∗ $p<0.01$).

to the free curcumin. The c-Myc and MMP7 protein, almost overexpressed in cancer cells, are related to cell proliferation, apoptosis, and invasion. The results that curcumin could decrease the expressions of c-Myc and MMP7, may explain the mechanism of the inhibitory effects on proliferation and invasion of metastatic osteo-

sarcoma 143B cells.

CONCLUSION

In this paper, a mixed system of mPEG-PLGA and PCL was used to build a formulation of curcumin-encapsulated polymeric nanoparticles, which greatly solved the limitations of free curcumin with intrinsic property of hydrophobicity and extreme instability. The encapsulation in the mPEG-PLGA/PCL significantly improved the solubility, stability and cellular uptake of curcumin. The Cur-NPs possess significantly higher inhibition for the proliferation, migration and invasion of osteosarcoma 143B cells than the free curcumin. It is found that both free curcumin and Cur-NPs could decrease the expressions of c-Myc and MMP7 in the level of mRNA and protein, which explained the mechanism of the inhibitory effects on proliferation, migration and invasion of metastatic osteosarcoma 143B cells. The Cur-NPs provide a promising strategy for metastatic osteosarcoma treatment.

Received 11 July 2017; accepted 27 August 2017; published online 27 September 2017

1 Kansara M, Teng MW, Smyth MJ, *et al.* Translational biology of osteosarcoma. Nat Rev Cancer, 2014, 14: 722–735
2 Grimer RJ. Surgical options for children with osteosarcoma. Lancet Oncology, 2005, 6: 85–92
3 Luetke A, Meyers PA, Lewis I, *et al.* Osteosarcoma treatment–Where do we stand? A state of the art review. Cancer Treatment Rev, 2014, 40: 523–532
4 Li Y, Rogoff HA, Keates S, *et al.* Suppression of cancer relapse and metastasis by inhibiting cancer stemness. Proc Natl Acad Sci USA, 2015, 112: 1839–1844
5 Benjamin RS. Osteosarcoma: better treatment through better trial design. Lancet Oncology, 2015, 16: 12–13
6 Kunnumakkara AB, Anand P, Aggarwal BB. Curcumin inhibits proliferation, invasion, angiogenesis and metastasis of different cancers through interaction with multiple cell signaling proteins. Cancer Lett, 2008, 269: 199–225
7 Heger M, van Golen RF, Broekgaarden M, *et al.* The molecular basis for the pharmacokinetics and pharmacodynamics of curcumin and its metabolites in relation to cancer. Pharmacol Rev, 2014, 66: 222–307
8 Cheng AL, Hsu HC, Lin JK, et al. Phase I clinical trial of curcumin, a chemopreventive agent, in patients with high-risk or pre-malignant lesions. Anticancer Res, 2001, 21: 2895–2900
9 Dhillon N, Aggarwal BB, Newman RA, *et al.* Phase II trial of curcumin in patients with advanced pancreatic cancer. Clin Cancer Res, 2008, 14: 4491–4499
10 Liu L, Sun L, Wu Q, *et al.* Curcumin loaded polymeric micelles inhibit breast tumor growth and spontaneous pulmonary metastasis. Int J Pharm, 2013, 443: 175–182
11 Gao X, Zheng F, Guo G, *et al.* Improving the anti-colon cancer activity of curcumin with biodegradable nano-micelles. J Mater Chem B, 2013, 1: 5778
12 Yallapu MM, Nagesh PKB, Jaggi M, *et al.* Therapeutic applications of curcumin nanoformulations. AAPS J, 2015, 17: 1341–1356
13 Chang Z, Xing J, Yu X. Curcumin induces osteosarcoma MG63 cells apoptosis *via* ROS/Cyto-C/Caspase-3 pathway. Tumor Biol, 2014, 35: 753–758
14 Chang R, Sun L, Webster TJ. Selective inhibition of MG-63 osteosarcoma cell proliferation induced by curcumin-loaded self-assembled arginine-rich-RGD nanospheres. Int J Nanomedicine, 2015, 1: 3351
15 Chen P, Wang H, Yang F, *et al.* Curcumin promotes osteosarcoma cell death by activating MiR-125a/ERRα signal pathway. J Cell Biochem, 2017, 118: 74–81
16 Walters DK, Muff R, Langsam B, *et al.* Cytotoxic effects of curcumin on osteosarcoma cell lines. Invest New Drugs, 2008, 26: 289–297
17 Jin S, Xu H, Shen J, *et al.* Apoptotic effects of curcumin on human osteosarcoma U2OS cells. Orthop Surg, 2009, 1: 144–152
18 Fossey SL, Bear MD, Lin J, *et al.* The novel curcumin analog FLLL32 decreases STAT3 DNA binding activity and expression, and induces apoptosis in osteosarcoma cell lines. BMC Cancer, 2011, 11: 112
19 Peng SF, Lee CY, Hour MJ, *et al.* Curcumin-loaded nanoparticles enhance apoptotic cell death of U2OS human osteosarcoma cells through the Akt-Bad signaling pathway. Int J Oncol, 2014, 44: 238–246
20 Fatima MT, Chanchal A, Yavvari PS, *et al.* Cell permeating nanocomplexes of amphiphilic polyelectrolytes enhance solubility, stability, and anti-cancer efficacy of curcumin. Biomacromolecules, 2016, 17: 2375–2383
21 Si M, Zhao J, Li X, et al. Reversion effects of curcumin on multidrug resistance of MNNG/HOS human osteosarcoma cells *in vitro* and *in vivo* through regulation of P-glycoprotein. Chin Med J, 2013, 126: 4116–4123
22 Dhule SS, Penfornis P, Frazier T, *et al.* Curcumin-loaded γ-cyclodextrin liposomal nanoparticles as delivery vehicles for osteosarcoma. Nanomed-Nanotech Biol Med, 2012, 8: 440–451
23 Luu HH, Kang Q, Park JK, *et al.* An orthotopic model of human osteosarcoma growth and spontaneous pulmonary metastasis. Clin Exp Metastasis, 2005, 22: 319–329
24 He N, Zhang Z. Baicalein suppresses the viability of MG-63 osteosarcoma cells through inhibiting c-MYC expression *via* Wnt signaling pathway. Mol Cell Biochem, 2015, 405: 187–196
25 Lin CY, Lovén J, Rahl PB, *et al.* Transcriptional amplification in tumor cells with elevated c-Myc. Cell, 2012, 151: 56–67
26 Dang CV. MYC on the path to cancer. Cell, 2012, 149: 22–35
27 Wu CH, van Riggelen J, Yetil A, *et al.* Cellular senescence is an important mechanism of tumor regression upon c-Myc inactivation. Proc Natl Acad Sci USA, 2007, 104: 13028–13033
28 Lin L, Zhang JH, Panicker LM, *et al.* The parafibromin tumor suppressor protein inhibits cell proliferation by repression of the c-myc proto-oncogene. Proc Natl Acad Sci USA, 2008, 105: 17420–17425
29 Kessenbrock K, Plaks V, Werb Z. Matrix metalloproteinases: regulators of the tumor microenvironment. Cell, 2010, 141: 52–67
30 Szarvas T, Becker M, vom Dorp F, *et al.* Matrix metalloproteinase-7 as a marker of metastasis and predictor of poor survival in bladder cancer. Cancer Sci, 2010, 101: 1300–1308
31 Hu XT, Zhang FB, Fan YC, *et al.* Phospholipase C delta 1 is a novel 3p22.3 tumor suppressor involved in cytoskeleton organization, with its epigenetic silencing correlated with high-stage gastric

cancer. Oncogene, 2009, 28: 2466–2475
32 Sakamoto N, Naito Y, Oue N, *et al.* MicroRNA-148a is down-regulated in gastric cancer, targets MMP7, and indicates tumor invasiveness and poor prognosis. Cancer Sci, 2014, 105: 236–243
33 Song N, Liu H, Ma X, *et al.* Placental growth factor promotes metastases of ovarian cancer through MiR-543-regulated MMP7. Cell Physiol Biochem, 2015, 37: 1104–1112
34 Han G, Wang Y, Bi W. c-Myc overexpression promotes osteosarcoma cell invasion *via* activation of MEK-ERK pathway. Oncol Res Feat Preclin Clin Cancer Therap, 2012, 20: 149–156
35 Song W, Tang Z, Li M, *et al.* Polypeptide-based combination of paclitaxel and cisplatin for enhanced chemotherapy efficacy and reduced side-effects. Acta Biomater, 2014, 10: 1392–1402
36 Song W, Tang Z, Lei T, *et al.* Stable loading and delivery of disulfiram with mPEG-PLGA/PCL mixed nanoparticles for tumor therapy. Nanomed-Nanotech Biol Med, 2016, 12: 377–386
37 Franken NAP, Rodermond HM, Stap J, *et al.* Clonogenic assay of cells *in vitro*. Nat Protoc, 2006, 1: 2315–2319
38 Yallapu MM, Khan S, Maher DM, *et al.* Anti-cancer activity of curcumin loaded nanoparticles in prostate cancer. Biomaterials, 2014, 35: 8635–8648
39 Tian J, Min Y, Rodgers Z, *et al.* Nanoparticle delivery of chemotherapy combination regimen improves the therapeutic efficacy in mouse models of lung cancer. Nanomed-Nanotech Biol Med, 2017, 13: 1301–1307
40 Wang Z, Tan J, McConville C, *et al.* Poly lactic-co-glycolic acid controlled delivery of disulfiram to target liver cancer stem-like cells. Nanomed-Nanotech Biol Med, 2017, 13: 641–657
41 Shen Y. Elastin-like polypeptide fusion for precision design of protein-polymer conjugates with improved pharmacology. Sci China Mater, 2015, 58: 767–768
42 Zhang Y, Xiao CS, Li MQ, *et al.* Co-delivery of doxorubicin and paclitaxel with linear-dendritic block copolymer for enhanced anticancer efficacy. Sci China Chem, 2014, 57: 624–632
43 Xu C, Tian H, Chen X. Recent progress in cationic polymeric gene carriers for cancer therapy. Sci China Chem, 2017, 60: 319–328
44 Wang J, Liu Y, Ma Y, *et al.* NIR-activated supersensitive drug release using nanoparticles with a flow core. Adv Funct Mater, 2016, 26: 7516–7525
45 Li D, Ma Y, Du J, *et al.* Tumor acidity/NIR controlled interaction of transformable nanoparticle with biological systems for cancer therapy. Nano Lett, 2017, 17: 2871–2878
46 Leung MHM, Kee TW. Effective stabilization of curcumin by association to plasma proteins: human serum albumin and fibrinogen. Langmuir, 2009, 25: 5773–5777
47 Cabral H, Matsumoto Y, Mizuno K, *et al.* Accumulation of sub-100 nm polymeric micelles in poorly permeable tumours depends on size. Nat Nanotech, 2011, 6: 815–823
48 Li Y. Realize molecular surgical knife in tumor therapy by nanotechnology. Sci China Mater, 2015, 58: 851–851
49 Zhen M, Shu C, Li J, *et al.* A highly efficient and tumor vascular-targeting therapeutic technique with size-expansible gadofullerene nanocrystals. Sci China Mater, 2015, 58: 799–810
50 Yang X, Li Z, Wang N, *et al.* Curcumin-encapsulated polymeric micelles suppress the development of colon cancer *in vitro* and *in vivo*. Sci Rep, 2015, 5: 10322
51 Wang YJ, Pan MH, Cheng AL, *et al.* Stability of curcumin in buffer solutions and characterization of its degradation products. J Pharm Biomed Anal, 1997, 15: 1867–1876
52 Kaur K, Kumar R, Mehta SK. Nanoemulsion: a new medium to study the interactions and stability of curcumin with bovine serum albumin. J Mol Liquids, 2015, 209: 62–70
53 Mohanty C, Acharya S, Mohanty AK, *et al.* Curcumin-encapsulated MePEG/PCL diblock copolymeric micelles: a novel controlled delivery vehicle for cancer therapy. Nanomedicine, 2010, 5: 433–449
54 Li C, Luo T, Zheng Z, *et al.* Curcumin-functionalized silk materials for enhancing adipogenic differentiation of bone marrow-derived human mesenchymal stem cells. Acta Biomater, 2015, 11: 222–232

Acknowledgements This work was supported by the National Natural Science Foundation of China (51520105004, 51673189, 51390484, 51403204, 51673185, 51473029 and 51503202), Science and Technology Service Network Initiative (KFJ-SW-STS-166), and the Chinese Academy of Sciences Youth Innovation Promotion Association.

Author contributions Wang G, Song W conceived and designed the reported research. Wang G mainly performed the whole experiments. Shen N provided related reagents. Yu H assisted to lyophilizate samples. Deng M, Tang Z and Fu X analyzed the data. Wang G wrote the manuscript. All authors discussed the results and commented on the manuscript. Tang Z revised the manuscript.

Conflict of interest The authors declare that there is no conflict of interest.

Guanyi Wang was born in 1990, a PhD candidate in Jilin university. Currently she is a joint PhD student in Professor Zhaohui Tang and Xuesi Chen's group. She is majoring in biochemistry and molecular biology. Her research interests mainly focus on anti-tumor therapeutics.

Zhaohui Tang was born in 1976. Currently he is a professor at the Key Laboratory of Polymer Ecomaterials, Changchun Institute of Applied Chemistry, Chinese Academy of Sciences. His research interests include fabrication of nano-medicine, anti-tumor therapeutics and industrial development of biodegradable medical polymer materials.

Xueqi Fu was born in 1960. Currently he is a professor at Edmond H. Fischer Signal Transduction Laboratory, School of Life Sciences, Jilin University. His research interests focus on the cell signal transduction and anti-tumor drug screening.

负载姜黄素的聚合物纳米粒子抑制转移性骨肉瘤细胞增值和迁移

王冠祎[1,2], 宋万通[2], 沈娜[2], 于海洋[2], 邓明琥[3], 汤朝晖[2*], 付学奇[1*], 陈学思[2]

摘要 骨肉瘤是一种高转移性的恶性肿瘤, 5年生存率不到20%. 姜黄素(Cur)具有治疗癌症的潜在功效, 但其自身水溶性和稳定性差等性质限制了其临床使用. 本文用聚乙二醇-聚(D, L-丙交酯-乙交酯)/聚(ε-己内酯)负载姜黄素形成纳米粒子, 可以改善姜黄素的水溶性、稳定性和细胞内吞. 与非负载的姜黄素相比, 姜黄素纳米粒子在抑制骨肉瘤细胞增殖和迁移方面显示出明显的优势. 研究结果表明, 姜黄素和其纳米粒子均可降低c-Myc和MMP7表达, 这可以很好地解释姜黄素纳米粒子抑制骨肉瘤细胞的机制.